Title

Photochemical studies of cis-[Ru(bpy)$_2$(4-bzpy)(CO)](PF$_6$)$_2$ and cis-[Ru(bpy)$_2$(4-bzpy)(Cl)](PF$_6$): Blue light-induced nucleobase binding.

Authors

de Sousa, Aurideia P
Carvalho, Edinilton M
Ellena, Javier
et al.

Publication Date

2017-08-01

DOI

10.1016/j.jinorgbio.2017.05.006

Photochemical studies of *cis*-[Ru(bpy)$_2$(4-bzpy)(CO)](PF$_6$)$_2$ and *cis*-[Ru(bpy)$_2$(4-bzpy)(Cl)](PF$_6$): Blue light-induced nucleobase binding

Authors: Aurideia P. de Sousa[a], Edinilton M. Carvalho[a], Javier Ellena[b], Eduardo H. S. Sousa[a], Jackson R. de Sousa[a], Luiz G. F Lopes[a], Peter C. Ford[c] and Alda K. M. Holanda[a]*

Affiliations:

a. Departamento de Química Orgânica e Inorgânica, Universidade Federal do Ceará Cx. Postal 12200, Campus do Pici s/n, CEP 60440-900, Fortaleza - CE, Brazil

b. Instituto de Física de São Carlos-USP, Cx. Postal 780, CEP 13560-970, São Carlos - SP, Brazil

c. Department of Chemistry and Biochemistry, University of California, Santa Barbara, CA 93106-9510, USA

*Corresponding author: Email: aldakarine@yahoo.com.br; Fax: +55 85 33669978

Keywords:

4-benzoylpyridine, carbon monoxide, guanine, metallodrug, photorelease, ruthenium.

Highlights:

1) Synthesis of *cis*-[Ru(2,2'-bipyridine)$_2$(4-benzoylpyridine)(CO)](PF$_6$)$_2$ (**I**).

2) Synthesis and structure of *cis*-[Ru(2,2'-bipyridine)$_2$(4-benzoylpyridine)Cl](PF$_6$)$_2$ (**II**).

2) Ultraviolet photolysis of **I** sequentially releases benzoylpyridine and CO.

3) Blue light photolysis of **I** releases only benzoylpyridine.

4) Blue light photolysis of **II** can replace the 4-benzoylpyridine with guanine.

Abstract

The ruthenium(II) compounds *cis*-[Ru(bpy)$_2$(4-bzpy)(CO)](PF$_6$)$_2$ **(I)** and *cis*-[Ru(bpy)$_2$(4-bzpy)(Cl)](PF$_6$) (**II**) **(**4-bzpy = 4-benzoylpyridine, bpy = 2,2'-bipyridine) were synthesized and characterized by spectroscopic and electrochemical techniques. The crystal structure of **II** was determined by X-ray diffraction. The photochemical behavior of **I** in aqueous solution shows that irradiation with ultraviolet light (365 nm) releases both CO and 4-bzpy leading to the formation of the *cis*-[Ru(bpy)$_2$(H$_2$O)$_2$]$^{2+}$ ion as identified by NMR and electronic spectroscopy. Carbon monoxide release was confirmed with the myoglobin method and by gas chromatographic analysis of the headspace. CO release was not observed when aqueous **I** was irradiated with blue light (453 nm). Changes in the electronic and ^{1}H NMR spectra indicate that **I** undergoes photoaquation of 4-bzpy to form *cis*-[Ru(bpy)$_2$(CO)(H$_2$O)]$^{2+}$. Blue light irradiation of aqueous **II** released the coordinated 4-bzpy to give the *cis*-[Ru(bpy)$_2$(H$_2$O)(Cl)]$^{2+}$ ion. When the latter reaction was carried out in the presence of the nucleobase guanine, Ru-guanine adducts were formed, indicating that the metal containing photoproduct may also participate in biologically relevant reactions. The photochemical behavior of I indicates that it can release either CO or 4-bzpy depending on the wavelength chosen, a feature that may have therapeutic application.

Keywords: photorelease; carbon monoxide; metallodrug; ruthenium

Introduction

There has been considerable interest in recent years regarding the use of photoactive metal complexes for therapeutic applications [1,2]. In this context, the ruthenium(II) bis(bipyridyl) complexes are well known for their photophysical and photochemical properties and have been explored for biomedical and biophysical applications [1]. Due to their synthetic versatility, these are good candidates for photo-activated prodrugs [2-5] with some being subjected to clinical and preclinical trials [6]. For examples, Turro and coworkers have explored the photo-uncaging of various ligands that have chemo-therapeutic activity from such platforms [10-12]. Etchenique and coworkers previously reported the photo-controlled release of a pyridine derivative bound to a ruthenium(II) bis(bipyridine) center. This ligand was 4-aminopyridine , which is neurochemical agent that blocks K^+ channels [7]. This lab has also prepared a series of other metal-based photoreleasing systems [8]. In a different approach, Sadler et al. [4] have described the photochemical and nucleobase binding properties of intermediates formed by photo-labilization of Cl^- from *cis*-$[Ru(bpy)_2(CO)Cl]^+$ and concluded that this strategy provides valuable leads for new photo-activated antitumor ruthenium complexes. However, Ru-Cl bond hydrolysis also occurs in the dark, rendering that compound less-specific for photo-drug applications.

The present work was initiated to examine how changing the ligand (L) in complexes of the type *cis*-$[Ru(bpy)_2(CO)L]^+$ changes the photochemical properties of these species. Here we describe the

synthesis, characterization and photochemical properties of the new complex salts *cis*-[Ru(bpy)$_2$(4-bzpy)(CO)](PF$_6$)$_2$ (**I**) and *cis*-[Ru(bpy)$_2$(4-bzpy)(Cl)](PF$_6$) (**II**), where 4-bzpy = 4-benzoylpyridine, a π-acceptor ligand. The ligand 4-benzoylpyridine was chosen because presents a more extended π -system in comparison to other pyridine ligands previously used in ruthenium-based NO donors, *cis*-[Ru(bpy)$_2$L(NO)]$^{n+}$ (L = pyridine, picoline, 4-acetylpyridine, isonicotinamide) [9, 10]. . Additionally, It was observed that blue light photolysis (453 nm) of either **I** or **II** leads to labilization of 4-bzpy, while near-UV photolysis (365 nm) of **I** also leads to CO release.

Carbon monoxide is a small molecule bioregulator in mammalian physiology that may play key roles in wound healing, cytoprotection during inflammation and prevention of ischemia/reperfusion injury [11, 12]. These properties have engendered interest in developing strategies for CO delivery to physiological targets including thermally and photochemically activated CO-releasing moieties (CORMs, [12] and photoCORMs [13-15], respectively). For the latter, using light as the trigger can define the location, timing and dosage of CO release. Although optimal transmission of light through mammalian tissue requires red or near infrared wavelengths, shorter wavelength excitation may have value in treatment of subcutaneous cancers [16, 17] and bacterial infections [20].

The metal containing product from photoreactions of a photoCORM may also be biologically active and offer some

therapeutic potential. One might draw inspiration from the action of cisplatin, which crosslinks with DNA purine bases. However, cisplatin use is dose-limited due to systemic toxicity, primarily to the kidney [18]. An alternative strategy would be to use complexes that are inactive in the dark but react with nucleobases upon irradiation [11,12]. In this context, it is notable the products generated upon photolysis of **II** display nucleobase binding properties.

Experimental Section

Materials: Ultrahigh purity water from a Millipore system (model: Millipore Direct Q® 3UV) was used throughout the experiments. $RuCl_3 \cdot xH_2O$, 4-benzoylpyridine and 2,2'-bipyridine were purchased from Sigma-Aldrich and used without further purification. *cis*-$[Ru(bpy)_2Cl_2]$ (**III**) was prepared according to a procedure described in the literature [19].

Synthesis of the complexes: *cis*-$[Ru(bpy)_2(4\text{-bzpy})(Cl)](PF_6) \cdot H_2O$ (**II**): A solution was prepared by mixing a sample of **III** (0.200 g, 0.41 mmol) and 4-benzoylpyridine (0.080g, 0.43 mmol) in a 1:1 ethanol/water solution (20 mL). This mixture was heated at reflux for 3 h. The resulting solution was concentrated by rotary evaporation to a volume of 10 mL. The solid **II** was precipitated by the addition of saturated aqueous NH_4PF_6 solution (2 mL), collected by filtration and washed with cold water. Yield = 87 %. IR (KBr disks, ν_{max}/cm^{-1}): 3117 (C-H); 1667 (C=O, ketone group); 1446 (C-N); ^1H NMR (500 MHz, d^6-acetone, δ): 8.62 (d, bzpy-$H^{21,21'}$, J = 5.50 Hz); 7.61 (d, bzpy-$H^{22,22'}$, J =

6.00Hz); 7.83 (d, bzpy-$H^{26,26'}$, J = 7.00 Hz); 7.52 (t, bzpy-$H^{27,27'}$, J = 7.70 Hz); 7.73 (t, bzpy-H^{28}, J = 6.90 Hz). Analysis: Calcd. for $C_{32}H_{27}ClF_6N_5O_2PRu$. Exp. (calc): C, 48.58 (48.34); H, 3.41 (3.42); N, 8.85 (8.81)%. We also report the X-ray crystal structure of this compound (see below)

cis-[Ru(bpy)$_2$(4-bzpy)(CO)](PF$_6$)$_2$·H_2O(**I**): The reaction was carried out in a Schlenk flask connected to a CO gas line. A sample of *cis*-$[Ru(bpy)_2(4\text{-bzpy})Cl]PF_6$ (0.100 g, 0.14 mmol) diluted in dimethylformamide (3.0 mL) was stirred under CO (1 atm) at 120 °C for 120 h. The solid was precipitated by the addition of saturated aqueous NH_4PF_6 solution (2 mL), collected by filtration and washed with cold water. Yield = 93%. IR spectrum (KBr disk, ν_{max}/cm^{-1}): 3117 (C-H); 1446 (C-N), 1665 (C=O, ketone group), 1962 (C≡O carbonyl ligand); ^{1}H NMR (500 MHz, acetone-d_6, δ): 9.10 (d, bzpy-$H^{21,21'}$, J = 5.50 Hz); 8.06 (d, bzpy-$H^{22,22'}$, J = 6.00 Hz); 7.89 (d, bzpy-$H^{26,26'}$, J = 7.00 Hz); 7.57 (t, bzpy-$H^{27,27'}$, J = 7.70 Hz); 7.76 (t, bzpy-H^{28}, J = 6.90 Hz). Analysis: Calcd. for $C_{33}H_{27}F_{12}N_5O_3P_2Ru$. Exp.(calc): C, 42.49 (42.50); H, 2.89 (2.92); N, 7.51 (7.51)%.

Instrumentation: Electrochemical experiments were performed in a BAS Epsilon 2 818 electrochemical analyzer from Bioanalytical Systems. These measurements were performed using millimolar solutions of the complexes in acetonitrile as solvent and tetrabutylammonium perchlorate (TBAP) 0.1 M as supporting electrolyte. A conventional three-electrode glass cell was used with glassy carbon (ca. 0.13 cm^2 geometrical area), Pt foil, and Ag/AgCl

(filled with acetonitrile containing 0.1 M TBAP) working, auxiliary and reference electrodes, respectively. The electrochemical experiments were conducted at room temperature.

FTIR spectra were recorded for compounds **I** and **II** in KBr pellets using an ABB Bomem FTLA 2000-102 spectrophotometer. NMR spectra were recorded using a Bruker AVANCE DPX500 spectrometer in acetone-d_6. Photoproducts formed upon irradiation of **I** and of **II** in DMSO-d6/D_2O (20/80, v/v) and DMSO-d6/D_2O (5/95, v/v) solutions, respectively, were characterized by recording their NMR and optical absorption spectra. Electronic spectra were recorded on a HP-8453 diode-array spectrophotometer**.**

X-ray diffraction studies of single crystals of **II** were carried out on an Enraf–Nonius Kappa CCD diffractometer, using Mo K(α) radiation (0.71073 Å). Data collection used the COLLECT program [20], and integration and scaling of the reflections were performed with the HKL Denzo-Scalepack system of programs [21]. Absorption corrections were carried out by using the multi-scan method [22]. The structure was solved by direct methods with SHELXS-97 [23]. The models were refined by full-matrix least-squares on F2 with SHELXL-97 [24]. All the hydrogen atoms were stereochemically positioned and refined with the riding model.

Photolysis experiments were carried out at room temperature in 1.0 cm path length quartz cells capped with rubber septa. The solutions were deaerated by bubbling argon prior to photolysis and stirred during irradiation. Simultaneous dark reactions were carried

out with identical solutions as controls. The UV-Vis spectra of the latter solutions showed these samples to be stable in the dark at least during the time scale of the photochemical experiments. Quantitative analysis of product formation and disappearance of the starting materials was carried out by monitoring the electronic spectral changes (see below).

Continuous photolysis was performed using a blue LED (λ_{max} = 453 nm) or with the output from a 200 W high pressure mercury lamp mounted on an Oriel optical train passed through an interference filter to isolate the mercury line at 365 nm. Lenses were used to collimate the light beam and a shutter was used to control the irradiation time. The light intensity was determined using chemical actinometry with potassium trisoxalatoferrate(III) [25, 26]. In general, incremental quantum yields determined from incremental spectral changes were plotted versus the percent reaction and extrapolated back to 0% reaction to minimize inner filter effects. A linear fit of these data over the first 25-30% of the reaction provided a y-intercept equal to the initial quantum yield. Each reported quantum yield is the average of, at least, three independent experiments. For the primary photoreaction of compound **I,** quantum yields were determined by plotting the incremental quantum yields for the absorbance decrease at 415 nm versus the elapsed irradiation time as shown in Supporting Information (SI) Figures S1 and S2, respectively. For the secondary photoreaction of **I** seen with 365 nm irradiation, the spectral changes were measured after 2 min of irradiation, when the primary reaction

was effectively complete. In this case, the quantum yield was determined by plotting the incremental quantum yields after the first 2 min as calculated from further absorbance decreases at 415 nm versus the elapsed irradiation time (SI Figure S3). For photolysis of compound **II**, the quantum yield was determined by plotting incremental quantum yields for the decrease of a band at 440 nm versus the elapsed irradiation time as shown in SI Figure S4.

Interaction with guanine: An NMR sample was prepared by dissolving 8.4 mg of **II** in 0.035 mL of DMSO-d6. To this was added a 0.665 mL aliquot of a guanine stock solution prepared by dissolving 24.8 mg of guanine in 5 mL of warm D_2O/NaOH (0.02 M) solution under stirring. The guanine stock solution was added dropwise with stirring to avoid precipitation of the compound. The reaction during 453 nm photolysis of the solution was followed by NMR and electronic spectra for 2 h until the photoreaction is complete. The photoproduct solution was then stirred for 24 h to react with guanine after which NMR and electronic spectra were again obtained.

Analysis of CO release: The myoglobin assay [28] was used to evaluate photochemical CO release from *cis*-$[Ru(bpy)_2(4\text{-bzpy})CO](PF_6)_2$. In this assay, conversion from deoxy-myoglobin (Mb) to carbonmonoxy-myoglobin (MbCO) was monitored using a Cary 5000 UV-Vis-NIR/Varian spectrophotometer. All experiments were carried out under anaerobic conditions using a glove box (COY laboratories). For a typical measurement, myoglobin was dissolved in 1000 μL of 0.1 M phosphate buffer (pH 7.3), resulting in a 48 μM solution, placed in a

1 cm quartz cuvette and degassed with argon. Subsequently, a 2X excess of sodium dithionite was added to convert met-Mb to deoxy-Mb. Due to the insolubility of **I** in aqueous buffer, a stock solution (~96 μM) was prepared in methanol, and a aliquot of this stock solution (1000 μL) plus PBS buffer were then added to the deoxy-Mb solution to give a total volume 4000 μL and a final solution containing **I (**24 μM**)**, myoglobin (12 μM) and dithionite **(**24 μM**)**. The cuvette was sealed with a plug to prevent escape of CO or reoxidation of the myoglobin. The solution was initially kept in the dark to study the stability of the complex in aqueous buffer and then was illuminated using UV light (350 nm) until no further spectral changes could be observed for several consecutive measurements. Illuminations were interrupted in regular intervals to record the optical absorption spectrum. A dark control experiment was performed under the same conditions. This procedure was also followed using blue light (453 nm); however, there was no evidence for CO release in the latter case.

GC Analysis of CO release: The experiment was carried out as follows: A sample of **I** (15 mg) in a DMSO/H_2O (20/80, v/v) solution under 1 atm of argon in a Schlenk cuvette was photolyzed for 2 h using 365 nm light. The solution was allowed to equilibrate with the gas phase by shaking repeatedly for 2-3 min. A 500 μL sample of the gas phase from the Schlenk cell was then removed with a gastight syringe and the CO content was determined by gas chromatography with thermal conductivity detection (GC-TCD) using a programmable

Agilent model 6890 GC with a 10 m Carbosieve packed column. The injection port was maintained at 50 °C and the detector at 250 °C. The carrier gas was helium at a flow of 7.3 $mL \cdot min^{-1}$. The column was maintained at 35 °C for 5 min, raised at 40 $°C \cdot min^{-1}$ to 250 °C and held for 45 min. Carbon monoxide is well resolved with this configuration and is detected with an elution time of ca. 8.0 min.

Results

Syntheses and characterizations: The complex salt *cis*-$[Ru(bpy)_2(4\text{-bzpy})(Cl)](PF_6)$ (**II**) was prepared and isolated from the reaction of *cis*-$[Ru(bpy)_2Cl_2]$ (**III**) with 4-benzoyl pyridine and characterized using NMR and infrared spectroscopy and elemental analysis. In addition, the X-ray crystal structure of **II** was obtained. The IR spectra of both showed bands characteristic of the ν(C=N) and ν(C=C) bonds for 4-bzpy and overlapping bands of the bpy ligand in the range of 1610–1400 cm^{-1}. A band at 1665 cm^{-1} is attributed to ν(C=O) of the ketone group of 4-bzpy that is absent in the IR spectrum of the precursor **III** (SI Figure S5).

The structure of **II** was confirmed by X-ray diffraction studies of crystals obtained by slow evaporation from methanol. Crystal data and structure refinement for this complex are summarized in Table 1 and the ORTEP projection is shown in the Figure 1. Selected bond lengths and angles are given in Table 2. The structure confirms the assignment of *cis* geometry of the chloride ligand in relation to 4-bzpy ligand suggested by the synthetic route. The Ru-N(bpy) bond lengths

for Ru-N1 (2.052), Ru-N2 (2.064) and Ru-N3 (2.074 Å), each are *trans* to a nitrogen ligand, are quite similar, while that of Ru-N4 (1.965), *trans* to a chloride, is somewhat shorter. These results are in agreement with structures determined for related complexes [27]. The presence of a single PF_6^- ion confirms that the ruthenium is in the Ru(II) oxidation state.

Complex **II** was further characterized by ^{1}H NMR and 2D COSY spectroscopy and this is analyzed in the Supporting Information (SI Figure S6). All 16 signals for the H's of the two bipyridines were observed suggesting all H atoms are magnetically non-equivalent[28, 29], as expected for the *cis*-$[Ru(bpy)_2(4\text{-bzpy})Cl]^+$ complex.

Table 1. Crystal data and structure refinement for *cis*-[Ru(bpy)$_2$(4-bzpy)(Cl)](PF$_6$) (**II**).

Empirical formula	$(C_{32}H_{25}N_5OClRu)^+ \cdot PF_6^-$
Formula weight	777.06
Crystal system	Monoclinic
Space group	$P2_1/c$
Temperature	293(2) K
Crystal size	0.3 x 0.2 x 0.1 mm^3
Unit cell dimensions	a = 11.42(4) Å
	b = 21.24(6) Å β= 99.8(2)°
	c = 15.31(6) Å
Volume	3660(23) Å^3
Z	4
Absorption coefficient	0.607 mm^{-1}
F(000)	1560
Reflections collected	23911
Independent reflections	5819 [R(int) = 0.0973]
Goodness-of-fit on F^2	1.015
Final R indices [I>2σ(I)]	R1 = 0.0809, wR2 = 0.1755
R indices (all data)	R1 = 0.2153, wR2 = 0.1945
CCDC ref number	1487399

[a] Data collection, data processing, structure solution and structure refinement, respectively.

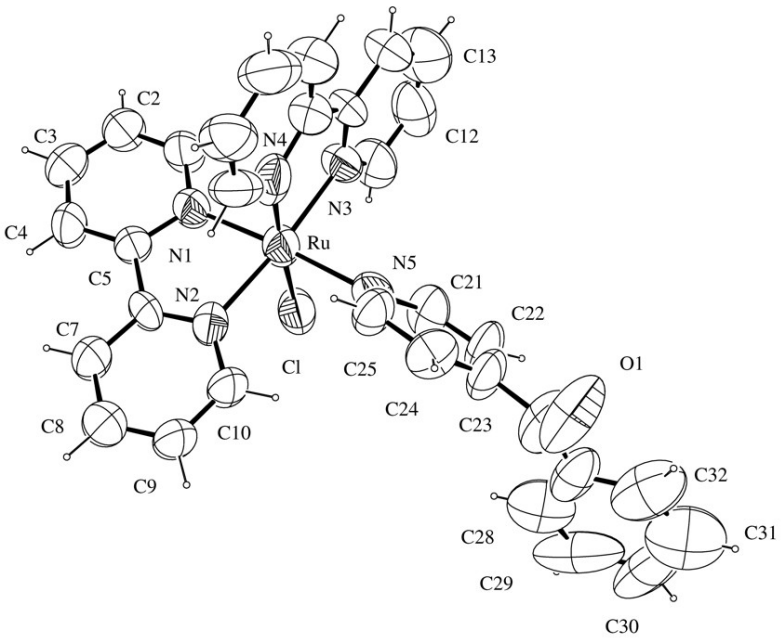

Figure 1. *ORTEP* [5] view of the complex cation of **II,** showing atom labeling and the 50% probability ellipsoids.

Table 2. Selected Bond lengths [Å] and angles [°] for *cis*-[Ru(bpy)$_2$(4-bzpy)(Cl)](PF$_6$) (**II**).

Bond lengths (Å)		Bond angles (°)	
Ru-N4	1.965(14)	N4-Ru-N1	91.2(3)
Ru-N1	2.052(9)	N1-Ru-N3	95.0(4)
Ru-N2	2.064(9)	N2-Ru-N3	174.4(4)
Ru-N3	2.074(10)	N2-Ru-N5	96.0(5)
Ru-N5	2.125(9)	N1-Ru-N5	176.0(3)
Ru-Cl	2.408(10)	N4-Ru-Cl	173.7(4)
N1-C1	1.351(10)	N2-Ru-Cl	86.3(3)
N1-C5	1.355(11)	N5-Ru-Cl	91.1(3)
N2-C6	1.327(11)	C1-N1-C5	116.6(8)
N2-C10	1.354(10)	C1-N1-Ru	128.3(8)
O1-C26	1.313(16)	C25-N5-Ru	118.9(9)
C22-C23	1.326(13)	O1-C26-C2)	122.5(17)
C23-C24	1.386(13)	O1-C26-C23	116.8(15)
C24-C25	1.396(12)	C27-C26-C23	120.5(16)
C26-C27	1.384(16)	C26-C27-C28	129.1(17)

The well-characterized complex **II** was used to prepare *cis*-[Ru(bpy)$_2$(4-bzpy)(CO)](PF$_6$)$_2$ (**I**) by reaction with CO. The IR spectrum of the isolated compound showed a strong ν(CO) band at 1962 cm^{-1} within the range noted for other Ru(II)-CO compounds [30, 31], confirming the presence of coordinated CO (SI Figure S-7). The IR spectrum of **I** also exhibited vibrational bands corresponding to the ν(C=N) and ν(C=C) modes of the 4-benzoylpyridine ligand with overlapping bands of the bipyridine ligands in the range of 1610–1400 cm^{-1} [32] and the strong band at 1665 cm^{-1} attributed to the ketone ν(C=O) of 4-bzpy, consistent with continued coordination of this ligand after exchange of chloride for CO, as is the elemental analysis.

Analogous bands are observed in the IR spectrum of **II** (SI Figure S7) and of other 4-bzpy complexes such as *fac*-[Re(Cl)(4-bzpy)$_2$(CO)$_3$] and *fac*-[Re(Cl)(4-bzpy)$_2$(CO)$_3$] [33].

The carbonyl complex **I** was further characterized by ^{1}H NMR, ^{13}C NMR, and HMBC (Heteronuclear Multiple-Bond Correlation) spectroscopy. Figure 2 illustrates the HMBC spectrum for *cis*-[Ru(bpy)$_2$(4-bzpy)(CO)](PF$_6$)$_2$, where ^{1}H nuclei are correlated to remote ^{13}C nuclei (two or three bonds away) in a 2D experiment via long-range heteronuclear J couplings ($^2J_{CH}$ and $^3J_{CH}$) [34]. This experiment shows CO resonances at low field (δ 194.30 and δ 200.48 ppm). Only the first is correlated with H's in neighboring bonds, and this was assigned to the ketone carbonyl of the 4-bzpy ligand. The signal at δ 200.48 ppm can be assigned to the CO ligand, whereas coordinated carbonyls typically appear in the ^{13}C NMR spectrum in the range of 180-250 ppm [4, 33, 35]. The cross peak between the ketone carbon and the peaks at δ 7.89 and δ 8.06 ppm observed in the HMBC experiment locates the two doublet signals of protons corresponding to H-29/H-33 and H-23/H-25, respectively, shown in Figure 2A. The ^{1}H NMR spectrum showed signals for the other hydrogens present in the 4-bzpy ligand, two triplets at 7.57 and 7.76 ppm, assigned to the H-30/H-32 and H-31, respectively. All the signals are shifted downfield from those observed for the free ligand. This effect is even more pronounced for H-22/H-26 (δ 9.10 ppm versus δ 8.81 in free), due to proximity to the ruthenium center. Additionally, the 16 signals seen for the bipyridine hydrogens indicate that all H's are magnetically

nonequivalent [36, 37] as expected for the *cis* configuration this cation.

Cyclic voltammetry (SI Figure S8) revealed quasi-reversible events with $E_{1/2}(Ru^{2+/3+})$ values of –0.11, 0.55 and 1.15 V vs Ag/AgCl (which would be the equivalent of 0.01, 0.56 and 1.34 vs Fc/Fc+) and ΔEp values of 0.10, 0.09 and 0.11 V for the respective complex compounds **III**, **II** and **I**. Replacing one chloride of *cis*-$[Ru(bpy)_2(Cl_2)]$ by the π-acceptor ligand 4-bzpy to give *cis*-$[Ru(bpy)_2(4\text{-bzpy})(Cl)]^+$ leads to an anodic shift of the redox potential by 0.66 V (-0.11 vs 0.55V). Replacing the second chloride by CO to give **I** leads to a further anodic shift of 0.60 V. Thus, these π-acceptor ligands (4-bzpy and CO) stabilize the ruthenium d-orbitals, and the Ru(II) center is much less readily oxidized.

B

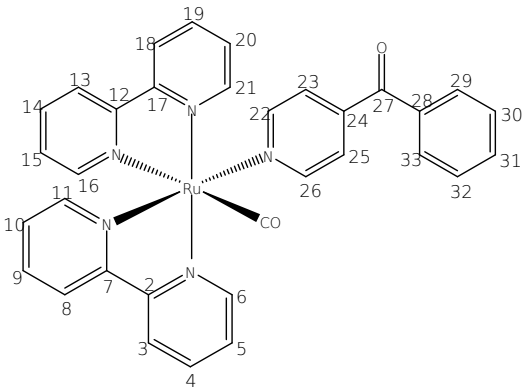

A

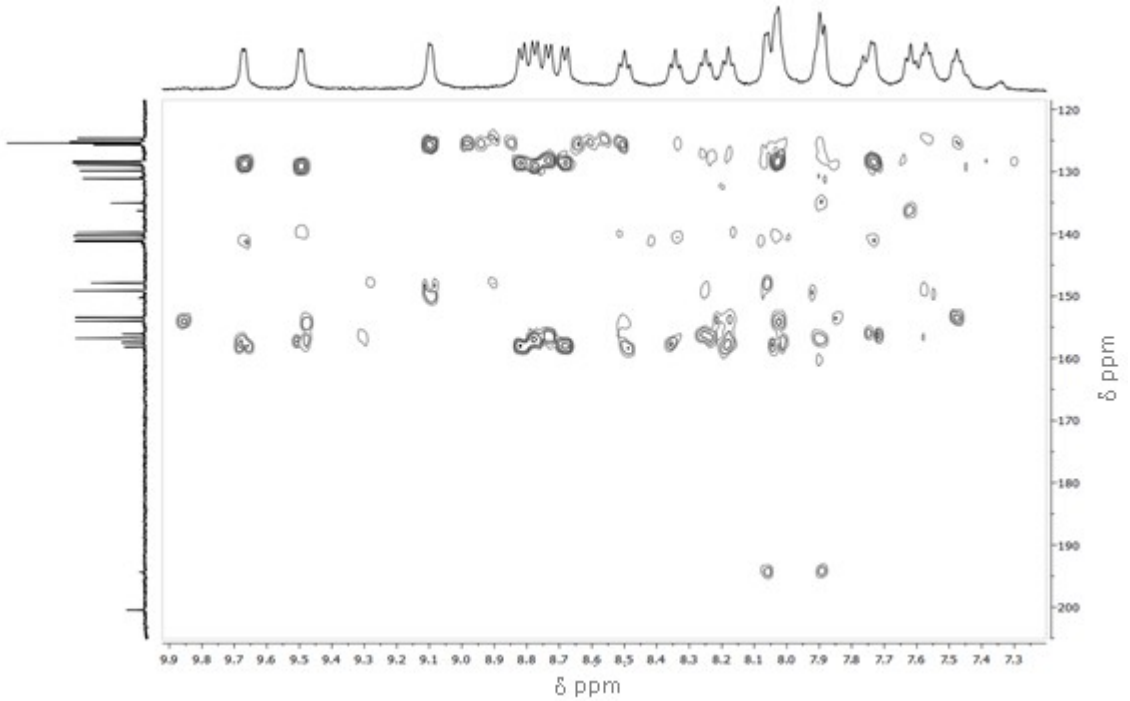

Figure 2. A) Drawing of *cis*-$[Ru(bpy)_2(4\text{-bzpy})(CO)]^{2+}$. B) HMBC spectrum of **I** in CD_3COCD_3.

The electronic absorption spectra of the *cis*-$[Ru(bpy)_2(4\text{-bzpy})L]^{+/2+}$ complexes in DMSO/H_2O (20/80, v/v) solution (SI Figures S9 and S10) display strong bands in the ultraviolet region and somewhat weaker bands in the visible. For **I** (L = CO), these bands occur at 274 nm (ε = 2.01 x 10^4 M^{-1} cm^{-1}), 303 nm (6.93 x 10^3 M^{-1} cm^{-1}) and 415 nm (5.90 x 10^3 M^{-1} cm^{-1}), while for **II** (L = Cl^-) analogous bands occur at 315 nm (ε = 2.20 x 10^4 M^{-1} cm^{-1}), 345 nm (7.93 x 10^3 M^{-1} cm^{-1}) and 440 nm (1.24 x 10^4 M^{-1} cm^{-1}). The UV absorption spectrum of free 4-bzpy displays a strong peak at 264 nm and a shoulder at 223 nm [38]. Although free 4-bzpy has a relatively low-lying nπ* excited state involving a ketone oxygen nonbonding orbital [33], these strong bands are $\pi^* \leftarrow \pi$ (4-bzpy) in origin. The higher energy strong bands observed in the spectrum for the *cis*-$[Ru(bpy)_2(4\text{-bzpy})L]^{+/2+}$

complexes are likely to be largely ligand localized transitions of the type (π*←π(bpy) , π*←π (4-bzpy), π*←n(4-bzpy) although these may overlap with π*(bpy)←dπ(Ru) metal to ligand charge transfer (MLCT) transitions. In analogy with other Ru(II) complexes [39, 40], the weaker visible range band seen for each complex can be assigned to a MLCT transition. Notably, this band occurs at higher energy for the carbonyl complex **I** than for the chlorido analog **II**. This effect can be attributed to the π*(CO)←dπ(Ru) backbonding interaction that stabilizes the dπ(Ru) orbitals in **I.**

Photochemical Studies: The photochemical behavior of **I** in DMSO/H_2O (20/80, v/v) solution was found to be complex, where there was no clear isosbestic point. From Figure 3, it is evident that the electronic spectra of photoproducts formed upon irradiation with blue light (λ_{irr} = 453 nm) (dotted line) and with UV light (λ_{irr} = 365 nm) (dashed line) are different. Photolysis with blue light leads to the appearance of a new absorption band at ca. 450 nm while UV photolysis gives a new band at 475 nm (Figure 3). Additionally, UV irradiation exhibited faster processes, where an apparent isosbestic point owing to faster photo-induced 4-bzpy release but this soon breaks down upon CO release. Thus, the product distribution from **I** is wavelength dependent. Furthermore, UV photolysis of **I** leads to CO release as demonstrated below, while no CO release was detected by the myoglobin test when an analogous solution was irradiated at 453 nm.

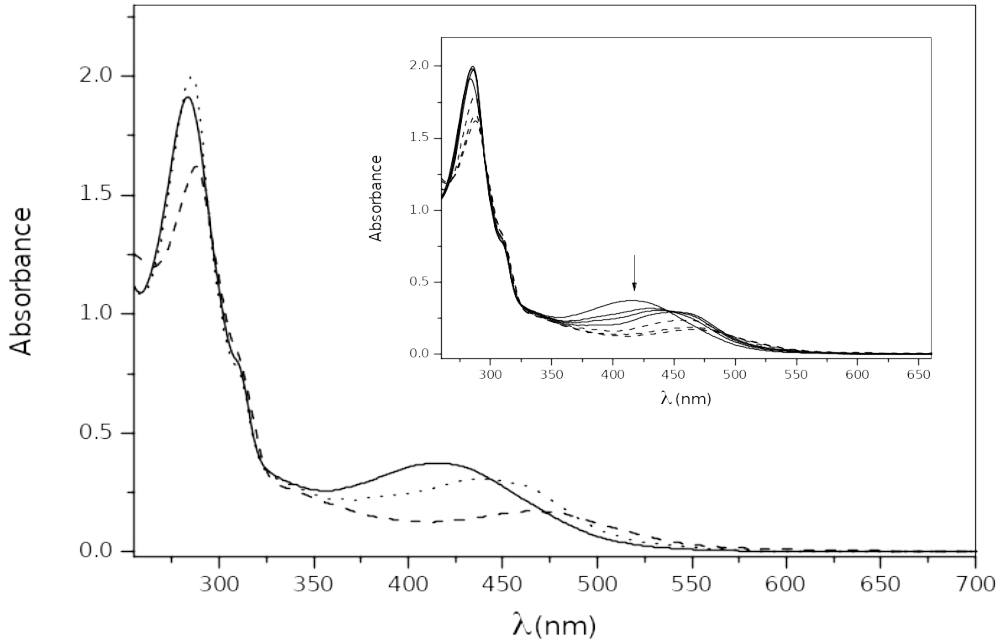

Figure 3. UV-visible spectra of *cis*-[Ru(bpy)$_2$(4-bzpy)(CO)](PF$_6$)$_2$ complex (**I**) in 20/80 DMSO/H$_2$O solution (6.42 x 10^{-5} M) as a function of photolysis. *Solid line:* before irradiation. *Dotted line*: after irradiation with blue light ($\lambda_{irr.}$ = 453 nm) for 2 h. *Dashed line*: spectrum after photolysis of **I** with 365 nm light for 2 h. *Inset:* Progressive spectral changes during the 365 nm photolysis of **I** in the same solvent over a period of 2 h (note: over time photolysis induced changes showed red shifts in the visible absorption bands as benzoylpyridine and CO are sequentially liberated.)

The temporal spectral changes upon photolysis of aqueous **I** with a blue LED showed a decrease in the MLCT absorption at 415 nm, the appearance of the new band at λ_{max} 450 nm with an isosbestic point at c.a. 450 nm (SI Figure S11) over the first 15 min, which supported initial release of 4-bzpy. Further photolysis for another 105 min led to no further changes. The absence of CO as a product and the general unreactivity of the bpy ligands toward photolabilization suggests that the visible light stimulated

photoreaction gives the monaqua species *cis*-$[Ru(bpy)_2(CO)(H_2O)]^{2+}$ (eq 1). The quantum yield ϕ_{bzpy} for this reaction was determined from the spectral changes to be 0.075 ± 0.003 (SI Figure S1).

$$cis\text{-}[Ru(bpy)_2(4\text{-}bzpy)CO]^{2+} \xrightarrow[H_2O]{\lambda_{irr.}=453\ nm} cis\text{-}[Ru(bpy)_2(H_2O)CO]^{2+} + 4\text{-}bzpy \quad (1)$$

The 365 nm irradiation of aqueous **I** displayed a different pattern of spectral changes. In the initial stage, the MLCT absorption at 415 nm decreases and the band at 450 nm becomes evident (Figure 3, inset) within 2 min of irradiation, similar to the pattern seen for the longer wavelength photolysis. This behavior suggests the formation of *cis*-$[Ru(bpy)_2(CO)(H_2O)]^{2+}$ as an intermediate. However, continued 365 nm photolysis is accompanied by evolution of the spectrum to give a new band with λ_{max} at 475 nm (Figure 3, inset, dashed line). The peak at 475 nm agrees with the spectrum of the diaqua complex *cis*-$[Ru(bpy)_2(H_2O)_2]^{2+}$ (**IV**) [41]. Thus, it appears that the intermediate aquo carbonyl complex undergoes secondary photolabilization of CO under continued UV photolysis (eq. 2). Under these conditions the quantum yield for the primary photoreaction was determined to be 0.095±0.003 (SI Figure S2), while that for the secondary reaction was determined to be ϕ_{CO} = 0.041 ± 0.004 (SI Figure S3).

$$cis\text{-}[Ru(bpy)_2(4\text{-}bzpy)CO]^{2+} \xrightarrow[H_2O]{\lambda_{irr.}=365\ nm} cis\text{-}[Ru(bpy)_2(H_2O)CO]^{2+} + 4\text{-}bzpy$$
$$\Big\downarrow \lambda_{irr.}=365\ nm,\ H_2O \qquad (2)$$
$$cis\text{-}[Ru(bpy)_2(H_2O)_2]^{2+} + CO$$

It should be noted that no spectral changes were observed when the solution of **I** was kept in the dark under similar experimental conditions. Alternatively, when the solution was photolyzed with blue light to give the spectrum of the intermediate -$[Ru(bpy)_2(CO)(H_2O)]^{2+}$ (**V**), there was no further spectral change upon storing for 24 h in the dark. This indicates that a second high energy photon is necessary for CO labilization from **V**.

With the aim of better characterizing the photoproducts, the ^1H NMR spectra of **I** in DMSO-d6/D_2O (20/80, v/v) were recorded before irradiation (Figure 4A), after irradiation with blue light (Figure 4B) and after irradiation with UV light (λ_{irr} = 350 nm) (Figure 4C). The aromatic region in the ^1H NMR spectrum before irradiation (Figure 4A) shows all the resonances from the non-equivalent sixteen protons of the two bpy ligands and five signals from the protons of the 4-bzpy ligand (δ 7.1-8.5) (SI Figure S12). Based on analogy to the ^1H NMR spectra of $[Os(bpy)_2(CO)(X)]^+$ (X = Cl, CF_3SO_3 or H) [42] and *cis*-$[Ru(bpy)_2(CO)Cl]^+$[4] the two lowest-field doublets (δ 9.31 and δ 9.22), can be assigned to the *ortho*-protons of the (bpy)pyridine rings *trans* each other. After irradiation with blue light (Figure 4B) the lowest-field doublet (δ 9.31) is shifted downfield to δ 9.45 and the second doublet (δ 9.22) is shifted upfield to δ 8.91. Analogous changes were observed by Sadler et al. [4] when *cis*-$[Ru(bpy)_2(CO)Cl]^+$ was irradiated with white light in DMSO-d6/D_2O (5/95, v/v) to give *cis*-$[Ru(bpy)_2(CO)(D_2O]^{2+}$. The ^1H NMR spectra of the blue light photoproduct from **I** is consistent with that of the latter species plus that

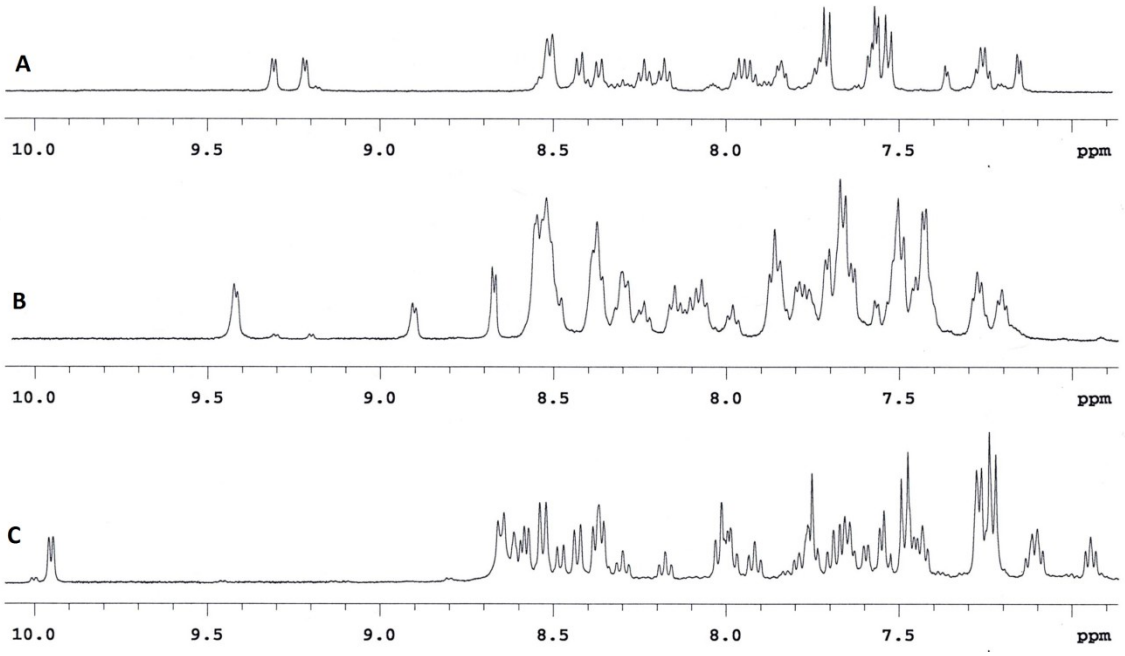

Figure 4. ^{1}HNMR spectrum of *cis*-[Ru(bpy)$_2$(4-bzpy)(CO)]$^{2+}$ in DMSO-d6/D_2O (20/80, v/v) solution. **A**: before irradiation. **B**: after 2 h irradiation with blue light (λ_{irr} = 453 nm). **C**: after 2 h irradiation with UV light (λ_{irr} = 365 nm).

of free 4-bzpy, which displays 5 resonances in the aromatic region, the most distinctive being at δ 8.65 (SI Figure S12). Thus the NMR spectra confirm that the principal photoreaction is 4-bzpy labilization according to eq. 1.

Figure 4C shows the ^{1}H NMR spectra of a solution of **I** after 2 h irradiation with UV light (λ_{irr} = 365 nm). This is clearly different to that shown in the Figure 4B for the photoproducts from irradiation with blue light. Comparing the ^{1}H NMR spectrum in Figure 4C with that of an authentic sample of *cis*-[Ru(bpy)$_2$(4-bzpy)H_2O]$^{2+}$(**VI**), which was prepared by reaction of *cis*-[Ru(bpy)$_2$(4-bzpy)NO]$^{3+}$ with NaN_3[43, 44] (SI Figure S13), shows that **VI** is not the photoproduct. Thus, since longer term UV irradiation of **I** leads to CO release, with no evidence

for formation of **VI**, we conclude both CO and 4-bzpy are released to form *cis*-$[Ru(bpy)_2(H_2O)_2]^{2+}$ according to eq. 2.

The release of CO as a photoproduct was confirmed using the myoglobin (Mb) assay method. Figure 5 shows the evolution of the spectrophotometric features of 12 μM of reduced MbFe(II) in PBS solution upon addition of 24 μM solution of the complex *cis*-$[Ru(bpy)_2(4\text{-bzpy})(CO)](PF_6)_2$ dissolved in methanol, followed by 350 nm irradiation of the solution. MbFe(II) was freshly obtained from native MbFe(III) upon addition of excess sodium dithionite (24 μM) inside an anaerobic chamber. Compound **I** proved to be stable in the dark for 24 h, but it released CO upon illumination at 350 nm. Upon irradiation for 2 h, the Q band at 557 nm related to MbFe(II) slowly disappeared, while bands at 540 and 577 nm characteristic of MbFeCO appeared [45]. The Soret band at 435 nm also showed the expected blue shift to 424 nm.

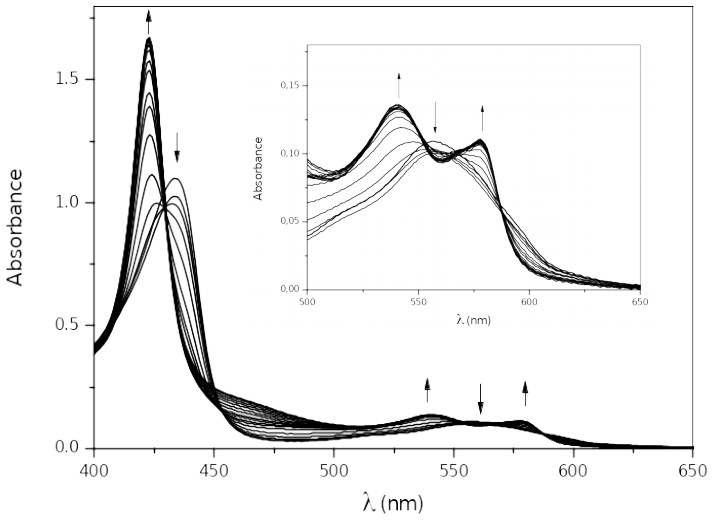

Figure 5. UV-visible spectra of freshly reduced 12 μM MbFe(II) in phosphate buffer solution upon addition of *cis*-$[Ru(bpy)_2(4\text{-bzpy})(CO)](PF_6)_2$ complex 24

μM, dissolved in methanol and irradiation with UV light (λ_{irr} = 350nm). *Insert*: Expansion in the region around Q bands (540 and 577 nm)[1]

In an independent experiment, the headspace over a solution of **I** was analyzed by GC-TCD after 365 nm irradiation, confirming the generation of free CO (SI Figure S14). In contrast, there was no CO detected in the Schlenk cuvette headspace after irradiation of *cis*-$[Ru(bpy)_2(4\text{-bzpy})(CO)]^{2+}$ at 453 nm. Quantification was achieved by comparison to a calibration curve determined for CO gas. The Schlenk cuvette has an internal volume of 30 mL and contained 4.0 mL of the photolysis solution. Given that CO has a solubility of 0.92 mM/atm in aqueous solution at 25 °C [47] (the temperature used in these experiments), one can calculate a partition coefficient of ~45/1 for CO between the gas and liquid phases at equilibrium. The product of the partition coefficient times the ratio of gas and liquid volumes (26/4) indicates that, at equilibrium, more than 99.5% of the CO generated will be in the gas phase of the Schlenk cuvette. The total CO released was calculated by taking into account this partitioning. Thus, by the GC methods, it was determined that a sample (15 mg) of **I** in DMSO/

[1] Fairlamb and co-workers [46] A.J. Atkin;, J.M. Lynam;, B.E. Moulton;, P. Sawle;, R. Motterlini;, N.M. Boyle;, M.T. Pryce;, I.J. Fairlamb, Dalton Transactions 40 (2011) 5755-5761. proposed that the myoglobin assay can be used to determine the amount of CO liberated from CO-RMs, but certain factors such as turbidity caused by poor CO-RM solubility or CO-RM absorbance, affect accurate calculation of Mb-CO concentrations. To overcome this problem, Motterlini and co-workers[45] R. Motterlini, J.E. Clark, R. Foresti, P. Sarathchandra, B.E. Mann, C.J. Green, Circ. Res. 90 (2002) 17-24. introduced the use of the isosbestic points at 510 nm as an internal reference for interconverting species (deoxy-Mb→Mb-CO). However, in the present case, it was not possible to observe the isosbestic points, possibly because the electronic spectrum of the *cis*-$[Ru(bpy)_2(H_2O)_2]^{2+}$ product shows a band in the same region (figure 3, dashed line). The overlapping bands makes the method ineffective for quantification of released CO.

H_2O (20/80, v/v) solution photolyzed for 2 h at 365 nm released 0.82±0.05 equivalents of CO per mole of complex.

Photolysis experiments were also performed with complex **II**. Electronic spectra changes during the photolysis with blue light in DMSO/H_2O (5/95, v/v) solution showed a decrease in the MLCT absorption at 440 nm and formation of a new band with a λ_{max} at 475 nm within 10 min (Figure 6). Further changes in the electronic spectrum were not observed even after 110 min additional photolysis or for a sample photolyzed for 30 min with blue light then stored in the dark for 24 h. In addition, there were no spectral changes for a DMSO/H_2O (5/95, v/v) solution of **II** kept in the dark under otherwise similar experimental conditions.

The photoreaction was also monitored by ^{1}H NMR spectroscopy (Figure 7). The ^{1}H NMR spectra of the photoproduct from blue light photolysis of **II** (Figure 7B) is not the same as that for the *cis*-$[Ru(bpy)_2(H_2O)_2]^{2+}$ (Figure 4C). Thus, the δ 8.65 signal indicates that the 4-bzpy ligand undergoes labilization to give the aqua species *cis*-$[Ru(bpy)_2(H_2O)Cl]^+$ (eq. 3), since this signal is observed in the ^{1}H NMR spectra for the free ligand 4-bzpy (SI Figure S12).

$$cis\text{-}[Ru(bpy)_2(4\text{-bzpy})Cl]^+ \xrightarrow[H_2O]{\lambda_{irr.}=453\ nm} cis\text{-}[Ru(bpy)_2(H_2O)Cl]^+ + 4\text{-bzpy} \quad (3)$$

Quantitative evaluation of photo-induced changes in the absorption spectrum gave the quantum yield for 4-bzpy photodissociation from **II** $\phi_{bzpy} = 0.131 \pm 0.005$ (SI Figure S4.

When a solution of **II** in DMSO/H_2O (5/95, v/v) was irradiated with 453 nm light in presence of 2 equivalents of guanine (G), the spectral changes were somewhat different. An initial decrease in the MLCT absorption of **II** at 440 nm was accompanied by the growth of a band at 475 nm over the first 30 min, consistent with formation of *cis*-$[Ru(bpy)_2(H_2O)Cl]^+$ (eq. 3). When the resulting solution is left in the dark for 24 h with stirring, the MLCT absorption at 475 nm decreased and a new absorption appeared at 510 nm (Figure 6-dashed line). This result suggests that the *cis*-$[Ru(bpy)_2(H_2O)Cl]^+$ photoproduct reacts with G to give the *cis*-$[Ru(bpy)_2(G)(Cl)]^+$, (eq. 4), although excess guanine was used in this experiment, we believe that only the mono adduct was formed. Earlier studies by Reedijk and co-workers showed that *cis*-$[Ru(bpy)_2Cl_2]$ forms only a N(7) mono adduct with 9-ethylguanine even under strong conditions and precipitation of the halides [[48].

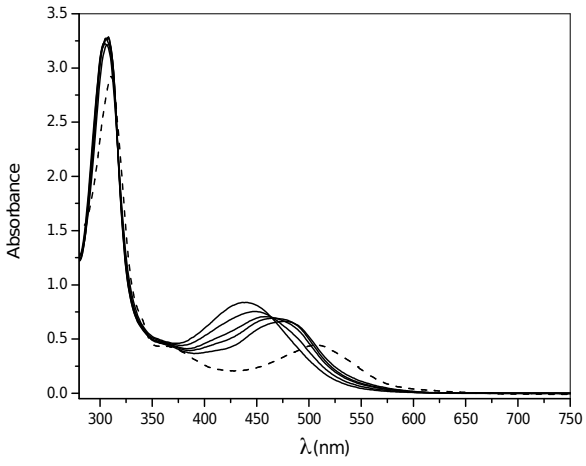

Figure 6. *Solid line*: Absorption spectra changes accompanying photolysis of **II** (1.18 x 10^{-4} M), in DMSO/H_2O (5/95, v/v) solution for 2 h, λ_{irr} = 453 nm. *Dashed line*: UV-vis spectra of **II** (1.18 x 10^{-4} M) after 453 nm irradiation in presence of 2 equivalents of guanine (G) in DMSO/H_2O (5/95, v/v) solution followed by leaving in the dark for 24 h with stirring.

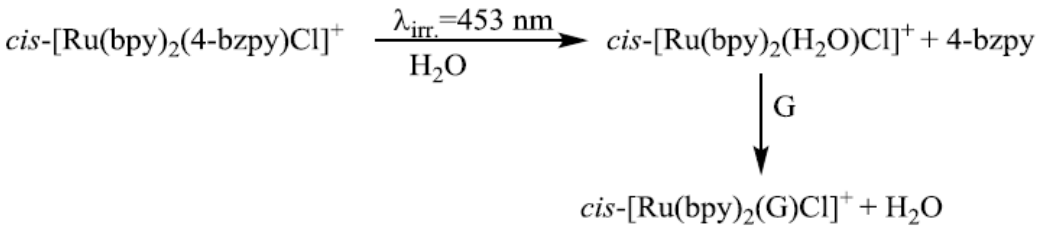

(4)

Figure 7 shows the ^{1}H NMR spectra obtained for a solution of **II** in DMSO-d6/D_2O (5/95, v/v) containing 2 equivalents of guanine before photolysis and after the solution was irradiated and left in the dark for 24 h. Only one type of metal-nucleobase was observed as revealed by appearance of a new singlet resonance at 6.41 ppm. This resonance can be assigned to the H8 of guanine in the N(7) Ru-guanine mono adduct, compared to free guanine which shows this at 7.40 ppm. This shift is consistent with the shielding effect induced by the ring current of the bpy ligands [13,[48].

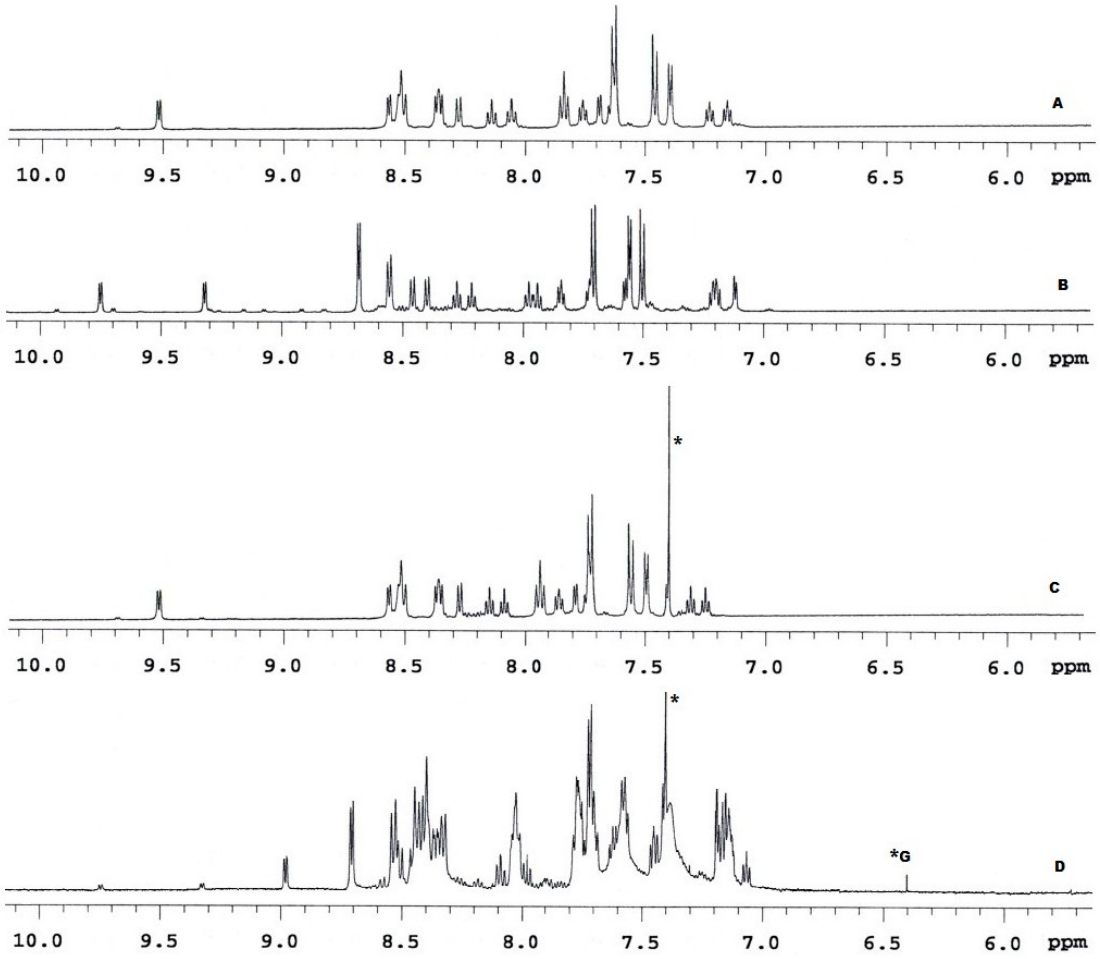

Figure 7. ^{1}H NMR spectrum of *cis*-[Ru(bpy)$_2$(4-bzpy)(Cl)](PF$_6$) in solution DMSO-d6/D$_2$O (5/95, v/v). A: before irradiation; B: after irradiation with blue light for 2 h; C: in presence of 2 equivalents of guanine (G) in the dark; D: in presence of 2 equivalents of guanine (G), after irradiation with blue light for 2 h and then left in the dark for 24 h under stirring. The asterisk (*) indicates H8 proton of free guanine and (*G) indicates H8 proton of guanine coordinated

Summary and Conclusions

We have prepared a CO-bound ruthenium complex **I** containing 4-benzoylpyridine aiming to controlled photorelease CO and also to generate potentially reactive ruthenium products. Interestingly, complex **I** quantitatively photoreleases CO upon UV (365 nm) irradiation, but not upon blue light (453 nm) irradiation. However, the 4-bzpy was photoreleased at either excitation wavelength. Complex

II, which does not contain CO was also able to photorelease 4-bzpy. Indeed, guanine was showed to bind to the ruthenium aquo species *cis*-$[Ru(bpy)_2(H_2O)Cl]^+$ generated by the latter photoreaction, suggesting that these complexes might interact with DNA, thereby mimicking a platinum-based drug. Along these lines, such dual or single ligand photorelease under controlled wavelengths might be further explored for therapeutic purposes.

Acknowledgments

The authors are thankful to Brazilian agencies CAPES, CNPq (L. G. F. Lopes 303732/2014-8; E. H. S. Sousa 312030/2015-0), FUNCAP (PPSUS 12535691-9) for financial support. We thank Zhi Li of UC Santa Barbara for his help with quantum yield measurements and with CO quantification.

Supporting Information: Figures S1 to S14.

References

[1] J.R. Lakowicz, Principles of Fluorescence Spectroscopy, Kluwer Accademic/Plenum Publishers,New York, 1999.

[2] T.S. Kamatchi, N. Chitrapriya, S.K. Kim, F.R. Fronczek, K. Natarajan, European Journal of Medicinal Chemistry 59 (2013) 253-264.

[3] C. Mari, V. Pierroz, S. Ferrarib, G. Gasser, Chemical Science 6 (2015) 2660-2686.

[4] L. Salassa, T. Ruiu, C. Garino, A.M. Pizarro, F. Bardelli, D. Gionolio, A. Westendorf, P.J. Bednarski, C. Lamberti, R. Gobetto, P.J. Sadler, Organometallics 29 (2010) 6703-6710.

[5] L. Salassa, E. Borfecchia, T. Ruiu, C. Garino, D. Gianolio, R. Gobetto, P.J. Sadler, M. Cammarata, M. Wulff, C. Lamberti, Inorganic Chemistry 49 (2010) 11240–11248.

[6] W. H. Ang, P.J. Dyson, European Journal of Inorganic Chemistry (2006) 4003-4018.

[7] L. Zayat, C. Calero, P. Albores, L. Baraldo, R. Etchenique, J Am Chem Soc 125 (2003) 882-883.

[8] L. Zayat, O. Filevich, L.M. Baraldo, R. Etchenique, Philos Trans A Math Phys Eng Sci 371 (2013) 20120330.

[9] M.G. Sauaia, F.D. Oliveira, A.C. Tedesco, R.S. da Silva, Inorganica Chimica Acta 355 (2003) 191-196.

[10] F.O.N. Silva, S.X.B. Araujo, A.K.M. Holanda, E. Meyer, F.A.M. Sales, H.C.N. Diogenes, I.M.M. Carvalho, I.S. Moreira, L.G.F. Lopes, European Journal of Inorganic Chemistry (2006) 2020-2026.

[11] T. Sjöstrand, Nature Reviews Drug Discovery 164 (1949) 580-581.

[12] R. Motterlini, L.E. Otterbein, Nature Reviews Drug Discovery 9 (2010) 728-743.

[13] R. D. Rimmer, H. Richter, P.C. Ford, Inorganic Chemistry 49 (2010) 1180-1185.

[14] R.D. Rimmer, A.E. Pierri, P.C. Ford, Coordination Chemistry Reviews 256 (2012) 1509-1519.

[15] U. Schatzschneider, British Journal of Pharmacology 172 (2015) 1638-1650.

[16] A. Radu, R. Conde, C. Fontolliet, G. Wagnieres, H.V. den Bergh, P. Monnier, Gastrointestinal Endoscopy 57 (2003) 897-905.

[17] L. Brancaleon, H. Moseley, Lasers in Medical Science 17 (2002) 173-186.

[18] M.H. Hanigan, P. Devarajan, Cancer Ther. 1 (2003) 47-61.

[19] B.P. Sullivan, D.J. Salmon, T.J. Meyer, Inorganic Chemistry 17 (1978) 3334-3341.

[20] Enraf-Nonius, COLLECT, Delft (1997-2000).

[21] Z. Otwinowski, W. Minor, Meth. Enzymol. 276 (1997) 307.

[22] R.H. Blessing, Acta Crystallographica Section A 51 (1995) 33-38.

[23] G.M. Sheldrick, Acta Crystallographica Section A 64 (2008) 112-122.

[24] G.M. Sheldrick, SHELXL-97., Program for Crystal Structures Analysis, University of Gottingen, Gottingen, Germany (1997).

[25] J.G. Calvert, J.N. Pitts, Photochemistry, J.Wiley and Sons,New York, 1967.

[26] G.A. Crosby, J.N. Demas, J. Phys. Chem. 75 (1971) 991-1024.

[27] D.A. Freedman, S. Kruger, C. Roosa, C. Wymer, Inorganic Chemistry 45 (2006) 9558-9568.

[28] R. Llanguri, J.J. Morris, W.C. Stanley, E.T. Bell-Loncella, M. Turner, W.J. Boyko, C.A. Bessel, Inorganica Chimica Acta 315 (2001) 53-65.

[29] M. Brissard, O. Convert, M. Gruselle, C. Guyard-Duhayon, R. Thouvenot, Inorganic Chemistry 42 (2003) 1378-1385.

[30] H. Ishida, K. Tanaka, M. Morimoto, T. Tanaka, Organometallics 5 (1986) 724-730.

[31] E. Fujita, Coord Chem Rev. 185-186 (1999) 373-384.

[32] N.C. Yumata, G. Habarurema, J. Mukiza, T.I.A. Gerber, E. Hosten, F. Taherkhani, M. Nahali, Polyhedron 62 (2013) 89-103.

[33] M. Busby, P. Matousek, M. Towrie, I.P. Clark, M. Motevalli, F. Hartl, A. Vlček Jr., Inorganic Chemistry 43 (2004) 4523-4530.

[34] D.L. Paiva, G.M. Lampman, G.S. Kriz, J.R. Vyvyan, Introduction to Spectroscopy, Cengage Learning,2009.

[35] T.R. Johnson, B.E. Mann, I.P. Teasdale, H. Adams, R. Foresti, C.J. Greenb, R. Motterlini, Dalton Transactions (2007) 1500-1508.

[36] R. Llanguri, J.J. Morris, W.C. Stanley, E.T. Bell-Loncella, M. Turner, W.J. Boyko, C.A. Bessel, Inorg. Chim. Acta 315 (2001) 53-65.

[37] M. Brissard, O. Convert, M. Gruselle, C. Guyard-Duhayon, R. Thouvenot, Inorganic Chemistry 42 (2003) 1378-1385.

[38] Y. Bai, G.S. Zheng, D.B. Dang, Y.N. Zheng, P.T. Ma, Spectrochim Acta A Mol Biomol Spectrosc. 79 (2011) 1338-1344.

[39] B. Durham, S.R. Wilson, D.J. Hodgson, T.J. Meyer, Journal of American Chemical Society 102 (1980) 600-607.

[40] D.M. Klassen, G.A. Crosby, J. Chem. Phys. 48 (1968) 1853-1858.

[41] B. Durham, S.R. Wilson, D.J. Hodgson, T.J. Meyer, Journal American Chemical Society 102 (1980) 600-607.

[42] R. Gobetto, C. Nervi, B. Romanin, L. Salassa, M. Milanesio, G. Croce, Organometallics 22 (2003) 4012-4019.

[43] D.W. Raichart, H. Taube, Inorganic Chemistry 11 (1972) 999-1002.

[44] T.J. Meyer, F.J. Miller, Journal American Chemical Society 93 (1971) 1294-1294.

[45] R. Motterlini, J.E. Clark, R. Foresti, P. Sarathchandra, B.E. Mann, C.J. Green, Circ. Res. 90 (2002) 17-24.

[46] A.J. Atkin;, J.M. Lynam;, B.E. Moulton;, P. Sawle;, R. Motterlini;, N.M. Boyle;, M.T. Pryce;, I.J. Fairlamb, Dalton Transactions 40 (2011) 5755-5761.

[47] R. Bartino, Iupac Solubility Data Series; Cargill, R. W., Oxford, U. K., 1990.

[48] P.M. van Wet, J.G. Haasnoot, J. Reedijk, Inorganic Chemistry 33 (1994) 1934-1939.